Research Square

Preprints are preliminary reports that have not undergone peer review.
They should not be considered conclusive, used to inform clinical practice,
or referenced by the media as validated information.

Preparation, Characterization, and CO2 Adsorption Performance of Activated Carbons Derived from Potato Peel Waste

Tuan-Dung Hoang
Vietnam National University, Hanoi
Minh-Thang Le
thang.leminh@hust.edu.vn

Hanoi University of Science and Technology

Research Article

Keywords: potato peel waste, biomass, activated carbons, pyrolysis, hydrothermal treatment, surface areas, adsorption

Posted Date: November 20th, 2026

DOI: https://doi.org/10.21203/rs.3.rs-11545110/v1

License: This work is licensed under a Creative Commons Attribution 4.0 International License.
Read Full License

Additional Declarations: No competing interests reported.

Preparation, Characterization, and CO_2 Adsorption Performance of Activated Carbons Derived from Potato Peel Waste

Tuan-Dung Hoang[1,2], Minh-Thang Le[3]*

[1] Vietnam National University, Hanoi, School of Interdisciplinary Sciences and Arts, 144 Xuan Thuy Street, Cau Giay District, Hanoi, 100000, Vietnam.

[2] Vietnam Aviation Academy, Faculty of Civil Engineering, 04 Nguyen Van Troi Street, Ward 8, Phu Nhuan District, Ho Chi Minh City, Vietnam.

[3]School of Chemistry and Life Sciences, Hanoi University of Science and Technology, No. 1 Dai Co Viet, Hai Ba Trung, Hanoi 113000, Vietnam.

*Author to whom correspondence should be addressed; email: thang.leminh@hust.edu.vn.

Abstract

The valorization of agro-industrial residues into porous carbon materials offers a sustainable approach to CO_2 capture. In this study, potato peel, an abundant biomass waste in Vietnam, was used as a precursor to prepare activated carbon by slow pyrolysis followed by KOH activation. Chemical activation substantially improved the textural properties, yielding a specific surface area of up to 969 m^2 g^{-1}. At 0 °C, the potato-peel-derived activated carbon exhibited a CO_2 uptake of approximately 1.78 mmol g^{-1}, higher than that of the corresponding okara-derived carbon (0.89 mmol g^{-1}), highlighting the importance of precursor-dependent pore development. NH_4OH treatment introduced nitrogen- and oxygen-containing surface functionalities, while CO_2 adsorption was strongly influenced by the development of narrow micropores. Overall, the results demonstrate that potato peel can be effectively converted into porous carbon adsorbents with promising CO_2 capture performance, highlighting the combined importance of pore structure and surface chemistry.

Keywords: potato peel waste, biomass, activated carbons, pyrolysis, hydrothermal treatment, surface areas, adsorption.

1. Introduction

Converting agricultural wastes into biochar and activated carbon for environmental remediation has been gaining attention lately due to this green approach [1, 2]. Potatoes (Solanum tuberosum L.) are among the top staple crops consumed globally, following wheat, rice, and maize. In 2013, global potato production reached 376 million tons [3, 4]. By 2024, it had increased to 383 million metric tons, with Asia accounting for 175.8 million and Europe for 47.2 million metric tons. Potato processing often generates significant peel waste, ranging from 15% to 40 %, depending on the peeling technique used [3]. This leftover material, known as potato peel waste (PPW), is abundant and low-cost. PPW is rich in starch, fibers (both starch and non-starch types), lignin, polyphenols, protein, and contains trace amounts of lipids [3]. Potato peel waste is generated from food processing activities, including potato chip manufacturing, fast-food chains, and household consumption in Vietnam. Although potato production in Vietnam is lower than that of staple crops such as rice or cassava, it is concentrated in key regions (e.g., the Red River Delta and Central Highlands), where processing activities produce considerable quantities of peel waste. Potato peel contains significant amounts of starch, cellulose, hemicellulose, and lignin, making it a promising precursor for activated carbon production. Its relatively high volatile content and porous structure after carbonization are advantageous for developing microporous carbon materials for gas adsorption applications. The general composition of potatoes includes about 2.1 % protein, 70 %–80 % water, 1.1 % fiber, 20.6 % carbohydrates, 0.3 % fat, and 0.9% ash [5].

Introducing basic functionalities, such as amine groups, into activated carbon structures can improve their chemical characteristics, basicity, and adsorption performance [6-8]. These groups can be incorporated using either wet or dry methods, depending on whether ammonia (NH_3) is applied in liquid or gas form at varied temperatures [9, 10]. This thermal treatment process—referred to as amination—is typically carried out between 200 °C and 800 °C [10]. During heating, ammonia decomposes into reactive radicals like NH_2, NH, hydrogen, and nitrogen atoms, which then form nitrogen-containing functional groups such as –CN, pyrrolic, and pyridinic structures when bonded to the carbon surface [10]. Adding NH_3 helps increase nitrogen content in activated carbon, thereby improving its affinity for acidic gases like CO_2 [6-8]. For example, Zhang [6] achieved a CO_2 capture capacity of 3.75 mmol/g at 1 atm and 20 °C using microwave treatment in a nitrogen atmosphere along with NH_4OH.

The impregnation of biochar/AC with NH_4OH can be attributed to several mechanisms. First, acid–base interactions occur between surface acidic groups (e.g., –COOH, –OH) and NH_3, which leads to the formation of ammonium salts such as $–COO^{-}\cdot NH_4^{+}$. In solution, NH_4^{+} ions generated in solution may be retained within the micropores of biochar through electrostatic forces or hydrogen bonding with oxygen-containing functional groups. Free NH_3 molecules can also interact with –OH/–C=O groups on the biochar/AC surface, or coordinate with residual inorganic components (like K, Ca, Mg, Al). Also, during drying or hydrothermal treatment, NH_4^{+}/NH_3 species may become confined within narrow pores or stabilized as ammonium complexes, enhancing their retention on the carbon surface [11]. Carboxyl (–COOH) or other acidic oxygenated groups deprotonate and interact with NH_4^{+}, supporting the following reaction [12], where R represents organic substituents:

$$RCOOH + NH_3 \leftrightarrow RCOONH_4^{+} \rightarrow RCONH_2 + H_2O$$

Similarly, Heidari [8] obtained up to 3.22 mmol/g at 1 bar and 30 °C using heat-modified ammonia solution. However, applying liquid-phase ammonia via wet impregnation may obstruct the activated carbon's porous network, potentially lowering its adsorption efficiency [6].

Biomass-derived activated carbons have attracted considerable attention as potential adsorbents for CO_2 capture because their textural properties and surface chemistry can be tailored through carbonization and activation [2, 13]. Previous studies have demonstrated that CO_2 adsorption performance depends on several factors, including the biomass precursor, specific surface area, pore-size distribution, micropore volume, and surface functional groups [14]. In particular, narrow micropores can enhance CO_2 adsorption through interactions between CO_2 molecules and the pore walls. However, the relationship between the preparation conditions, resulting pore structure, and CO_2 adsorption performance remains strongly dependent on the precursor and synthesis route [14]. Further investigation of locally available biomass residues is therefore valuable for understanding how these factors influence adsorption behavior. In this context, potato peel waste represents a potential precursor for producing porous activated carbon, although its suitability for CO_2 capture requires further systematic characterization and evaluation.

Results from previous studies consistently indicate that microporosity, surface areas, and functional groups play an important role in CO_2 uptake capacity. Activated carbons (AC) prepared

at optimized carbonization and activation temperatures often exhibit high specific surface areas and well-developed micropore volumes, which are favorable forCO_2 uptake under ambient or mildly elevated pressures [15] .

Despite these advances, most studies on biomass-derived activated carbons for CO_2 capture have primarily focused on material preparation and equilibrium adsorption capacity, while the relationships between surface properties, pore characteristics, and CO_2 adsorption performance remain insufficiently understood [15-17]. In particular, systematic investigations of how biomass precursor type and chemical modification affect the textural and surface properties of activated carbons and, consequently, their CO_2 adsorption capacity are still limited. In addition, the potential of low-cost agricultural and food-processing residues as precursors for developing effective CO_2 adsorbents has not been sufficiently explored comparatively. Therefore, further research is needed to establish clear relationships between precursor characteristics, activation/modification conditions, physicochemical properties, and CO_2 adsorption performance, thereby providing a better basis for the development of low-cost biomass-derived activated carbons for CO_2 capture.

2. Materials and Methods

The activated carbons were prepared according to Figure 1.

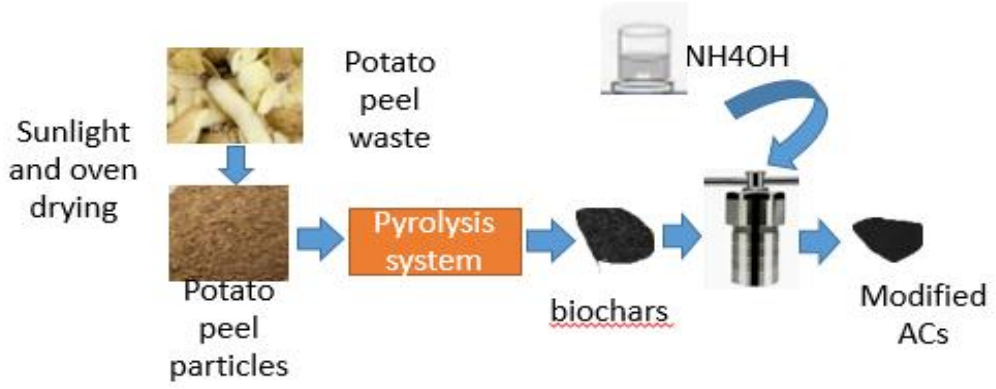

Figure 1. Schematic diagram of the bio-sorbent preparation

The base-modified activated carbons derived from potato peel waste were prepared following the same activation and base-modification procedures described above for the okara-derived activated carbons [14]. In contrast, Sample P2 underwent a 24-hour hydrothermal process at 200 °C, using a P1 as the precursor. The heating rate was maintained at 1 °C/min, with 75 mL

of ammonium hydroxide (NH_4OH) serving as the treatment medium. Sample P3 underwent a longer 48-hour hydrothermal treatment under the same temperature and heating rate, in a similar sized autoclave. Sample P4 was treated for an extended 72-hour period at 200 °C though the same reactor. Details of these samples are provided in the Table 1 below:

Table 1. Activated carbon sample preparation and treatment

Sample code	**Sample feedstock**	**Preparation details**
Potato peel waste feedstock	P1	pyrolysis at 600 ^oC; N_2 flow, 1 hour.
P2	P1	0.5g P1 mixed with 75 mL of NH_4OH solution; put into medium size autoclave; Hydrothermal experiment for 24 hours; at 200 ^oC; heating rate 1 $^oC\ min^-$
P3	P1	0.5g P1 mixed with 75 mL of NH_4OH solution; put into an autoclave of medium sizes; Hydrothermal experiment for 48 hours; at 200 ^oC; heating rate of 1 $^oC\ min^{-1}$
P4	P1	0.5 gr P1 mixed with 75 mL of NH_4OH solution; put into autoclave of medium size. Hydrothermal experiment sample for 72h; at 200 ^oC; heating rate 1 $^oCmin^{-1}$

Characterization of the materials

Transmission Electron Microscope (TEM) analysis is used to examine the pore structure of the AC samples. The TEM instrument is JEM2100, manufactured by JEOL. It operates at an acceleration voltage of 200 kV. Thermogravimetric analysis TGA-MS is used to monitor the weight change of a sample over time or as temperature increases. In this study, thermal behavior was assessed using a Netzsch STA 449 F5 Jupiter analyzer. Nitrogen gas was employed as the carrier at a flow rate of 50 mL/min, and the temperature was increased from ambient up to 800 °C.

The surface area, pore volume, and pore diameter of the activated carbon samples were assessed using nitrogen adsorption–desorption data collected at 77 K. These measurements were obtained using a Micromeritics Gemini VII 2390 analyzer (USA). The surface area was calculated using the Brunauer–Emmett–Teller (BET) equation over a relative pressure (P/P_0) range of 0.05 to 0.35. The total pore volume was determined from the nitrogen uptake at a relative pressure near saturation ($P/P_0 \approx 0.99$). Prior to the adsorption measurement, the sample was degased in a nitrogen flow at an elevated temperature of 300 ^oC for 3- 5 h until moisture was completely removed.

A Raman instrument, Horiba's Xplora Plus, was employed to identify the carbon type and to investigate and evaluate the structure and characteristics of the synthesized activated carbons.

X-ray diffraction (XRD) analysis is used to determine structural aspects such as phases, crystallite dimensions (D), and lattice strain (ε) of materials. Analyses were performed by a D8 Advance Bruker diffractometer Bruker, Germany, Cu Kα, 40 kV, 40 mA generator, NaI scintillation detector. The analysis conditions included Cu Kα with a wavelength of 15406 nm and a scanning range of 2 thetas from 10 – 80°. The database provided with the instrument is ICCD-PDF2. The XRD system was calibrated for θ and 2θ angles using corundum (Al2O3) as the standard.

CO_2 Temperature-Programmed Desorption (TPD-CO_2): TPD was employed to investigate surface interactions, including identification of basic/acidic sites and adsorbed compounds. The analysis was conducted using a Micromeritics AUTOCHEM–2950 system (USA), which was paired with a mass spectrometer. A 1.00 mg sample was loaded into a quartz reactor inside a stainless steel heating block. Initially, the sample was degassed under a helium (99.99%) stream at 300 °C for 15 minutes with a 3 °C/min heating rate. After cooling to 50 °C, CO_2 adsorption was performed using a 10% CO_2/He mixture. For desorption, the temperature was raised to 500 °C at 10 °C/min and held for 30 minutes

CO_2 adsorption measurements: CO_2 adsorption measurements of the ACs derived from potato peel were performed using a Micromeritics Gemini VII 2390 analyzer (USA). Before measurement, the samples were degassed under a nitrogen flow at 150 °C for 3–5 h to remove moisture and other adsorbed species. CO_2 adsorption experiments were subsequently conducted at

room temperature under elevated pressure, and the adsorption period was recorded to evaluate the adsorption behavior of the samples.

CO_2 capture and conversion experiment: A CO_2 adsorption–conversion experiment was conducted using the NH_4OH-modified activated carbon prepared from potato peel waste. The sample modified with NH_4OH for 48 h (P3) was selected for this experiment. Approximately 0.101 g of P3 was exposed to a continuous CO_2 stream at a flow rate of 50 mL min^{-1} for 2 h. Following CO_2 adsorption, the resulting carbon sample was collected and denoted as P3-deCO_2-1.

To investigate the subsequent conversion of the captured CO_2, the P3-deCO_2-1 sample was contacted with 100 mL of aqueous NaOH solution containing 0.4 g of NaOH. The suspension was maintained at 80 °C and continuously stirred for 45 min. After treatment, the solid phase was separated from the solution by vacuum filtration and dried in an oven at 100–110 °C until a constant mass was obtained. The dried solid was designated as P3-2.

The filtrate obtained after solid–liquid separation was subsequently concentrated by evaporation at 140 °C. The remaining solid residue was further dried at 100–110 °C for 24 h and designated as R1. The recovered solid products were subsequently characterized by Fourier-transform infrared spectroscopy (FTIR) to examine the formation of carbonate-containing species resulting from CO_2 conversion in the NaOH medium.

3. Results and Discussions

3.1. Characterization of AC material from potato peels

The potato peel-derived AC showed a surface area of 969.09 m^2/g, surpassing many other biomass precursors. Its total pore volume is 0.836 cm^3/g; the average pore width of 25.11 Å indicates mainly a mesoporous structure, which may enhance accessibility to internal adsorption sites.

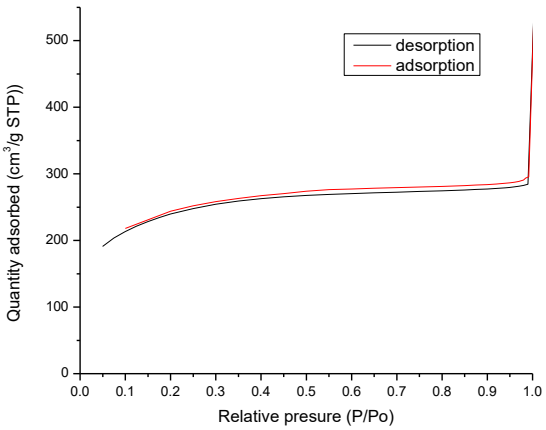

Figure 2. Isotherm linear plot of the original potato-derived AC sample

Figure 2 is the isotherm linear plot of the original potato-derived AC sample. The figure shows the adsorption isotherm, where the adsorbed quantity increases rapidly at low relative pressure ($P/P_0 < 0.2$) and reaches a plateau gradually at higher pressures. The figure also suggests the presence of micropores dominating uptake at low P/P_0, followed by pore filling at higher relative pressures.

The pore size distribution of the sample can be evidenced in Figure 3. The figure shows a dominance of mesopores, concentrated at about 25 Å can be observed. Compared to AC derived from okara [14], AC from potato peels showed a slightly larger pore size.

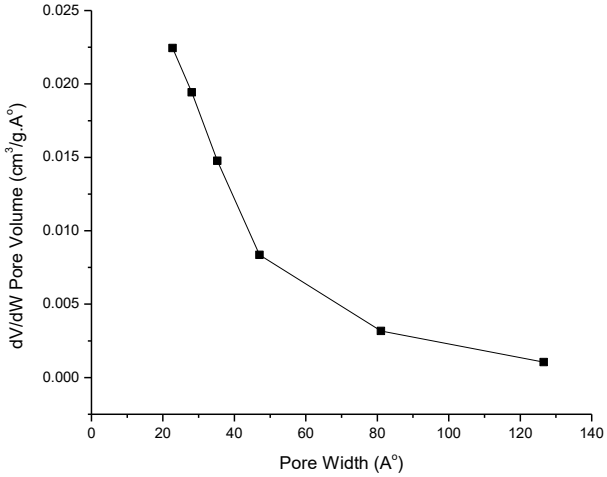

Figure 3 The pore distribution of potato-derived AC sample

TEM images of Potato-derived AC are presented in Figure 3. It is found out that potato-derived activated carbons consist of irregularly shaped carbon particles with a predominantly amorphous structure. AC exhibited pores of approximately 1 nm. Lattice fringes are absent in the sample, and this confirms the largely disordered nature of the carbon framework, which is typical for bio-derived activated carbons and favorable for gas adsorption applications [18].

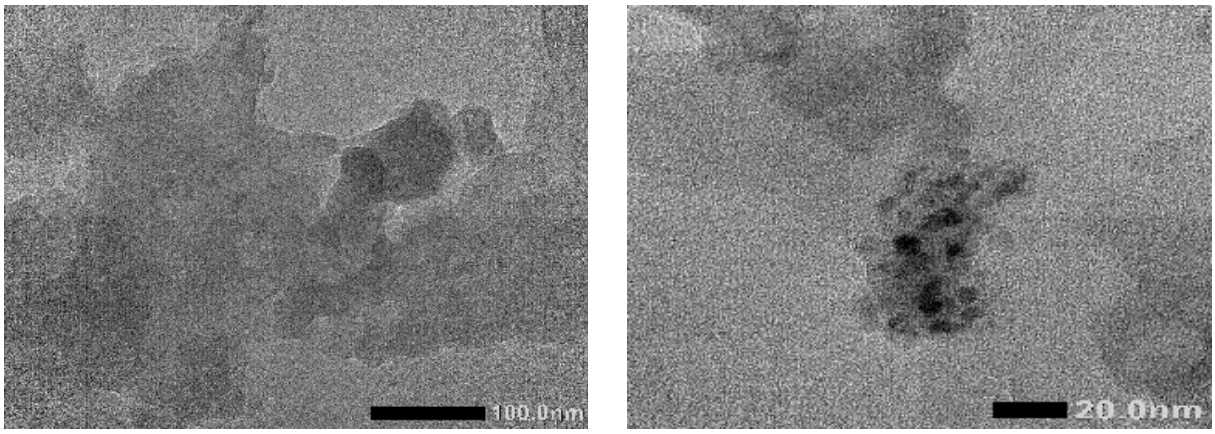

Figure 4. TEM (measured at 200x magnification) analysis of potato-derived AC.

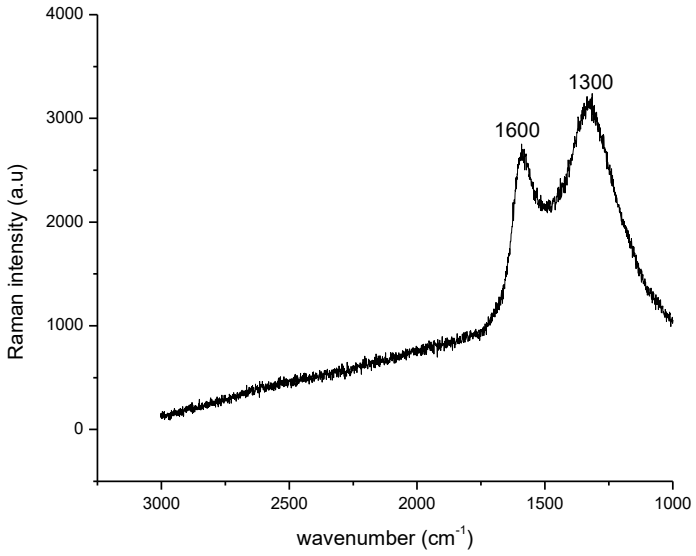

Figure 5. Raman spectra of AC derived from potato peels (P1)

Figure 5 presents the Raman spectra of activated carbon derived from potato peels. The activated carbon sample displays distinct peaks near 1300 cm^{-1} and 1600 cm^{-1}, which indicate the formation of AC. These peaks reflect the molecular structure characteristics of amorphous carbon [19].

The D-band, around 1350 cm^{-1}, arises from the breathing vibrations of aromatic rings and signifies the presence of disordered carbon or defects in the sp^2 carbon lattice, often linked to edge defects, functional groups, or amorphous carbon. The G-band, near 1580 cm^{-1}, is associated with the in-plane vibrations of sp^2-bonded carbon atoms, indicating the graphitic or ordered carbon structure. Although the sample lacks strong graphitic signals, the presence of graphite-like patterns suggests a well-developed porous structure in the synthesized activated carbon [19]. In addition, there are no prominent peaks observed beyond the G-band region (beyond 2000 cm^{-1}), suggesting minimal presence of overtone or combination modes, and supporting the conclusion that the material is primarily amorphous with low graphitic crystallinity. It is also worth noting that the scattered outlier points (above 4000 % intensity) are likely artifacts or noise and do not correspond to Raman-active modes, thus should be disregarded in structural interpretation.

The XRD pattern of the unmodified AC derived from potato peels is displayed in Figure 6. The pattern is characterized by Bragg reflection peaks at 2θ angles of 10.5º, 23.15º, and 44.5º, corresponding to the (002) and (100) planes of AC.

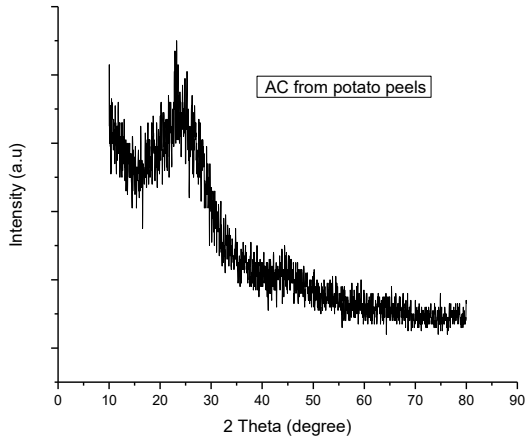

Figure 6. X-ray diffraction pattern of the activated carbon synthesized from potato peels (P1)

Broad peak at ~23º–25º corresponds to the (002) plane of disordered graphitic carbon, indicating the presence of amorphous carbon structure, not well-ordered graphite, which is typical for the amorphous structure of disordered graphite materials. No sharper peaks are observed, potentially indicating the presence of no crystalline inorganic components inside the sample.

Overall, the XRD analysis confirms that the materials are predominantly amorphous or poorly crystalline in nature [20].

Figure 7 a presents the SEM micrographs of the unmodified AC made from potato peels. The surfaces of all activated carbon samples reveal noticeable porosity. Before undergoing hydrothermal processing (Figure 7 a, at 1000x magnification), the sample shows pronounced and well-defined surface features. After hydrothermal treatment (Figure 7 b – d), the samples exhibit uneven and varied surface morphology, with coarse textures, fractured segments, and distinct porous characteristics.

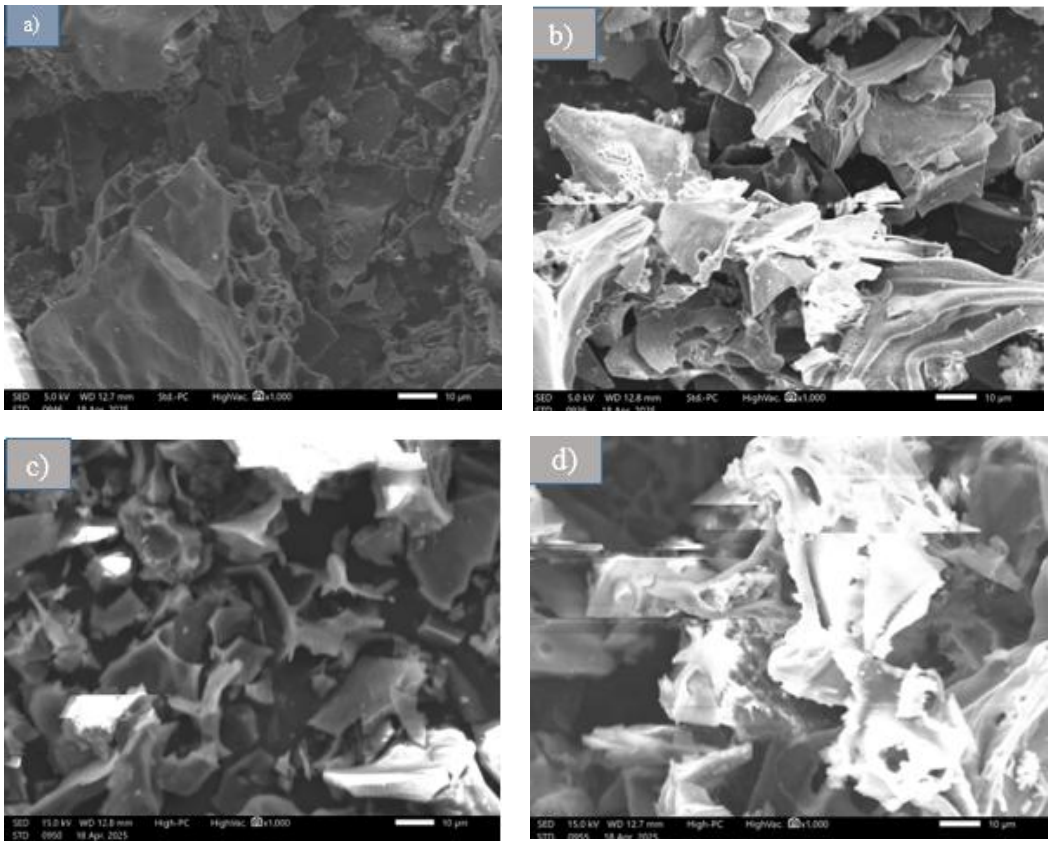

Figure 7. SEM images of samples (a) P1-Original AC, (b) P2–AC-NH_4OH-24h, (c) P3-AC-NH_4OH-48h, and (d) P4-NH_4OH-72h.

3.2. Characterization of potato peels-derived AC with NH_4OH impregnation

Figure 7 b-d presents the SEM micrographs of potato peels-derived AC with NH_4OH Impregnation. Visually, the original AC (P1) exhibits a relatively smooth and compact surface with fewer visible pores or surface irregularities, indicating minimal surface etching or

development of porosity. After 24 hours of NH_4OH treatment (P2), the surface begins to show slight etching and increased roughness. Small pores and cracks start to emerge, suggesting initial activation and surface modification. With 48 hours of treatment (P3), the surface roughness significantly increases. Numerous pores of varying sizes become apparent, and the structure appears more porous and fragmented. This indicates enhanced chemical activation and development of a higher surface area. Prolonged treatment for 72 hours (P4) leads to a highly porous and rough surface, with more extensive pore development and surface fragmentation. However, excessive etching might cause partial structural collapse or merging of pores, leading to larger but less uniform pore structures.

Comparatively, the carbon samples a) and c) present clear and deep textures, while samples b) and d) show more porous structures; overall morphology of b) and d) remains largely similar, retaining its rough and uneven characteristics. From figure a) to figure b), relatively significant structural changes are apparent at this 1000 magnification. The change in topography shows a potential interaction among elements on the surface area with NH_4OH addition and hydrothermal experiment conditions

The elemental profiles of the AC samples (P1 to P4) are summarized in Table 2 below. The original carbon (P1) consists primarily of carbon (85.66% by mass and 90.07% by atoms) and oxygen (10.86% mass, 8.57 % atom).

Table 2. EDX results of 4 samples derived from potato peels with NH_4OH impregnation

Element	**P1 (Original AC)**	**P2 (24 h NH_4OH)**	**P3 (48 h NH_4OH)**	**P4 (72 h NH_4OH)**
C (Mass/Atom %)	85.66 / 90.07	71.39 / 82.53	59.01 / 74.74	64.77 / 78.43
N (Mass/Atom %)	-	0.45 / 0.45	2.16 / 2.35	0.99 / 1.03
O (Mass/Atom %)	10.86 / 8.57	14.23 / 12.35	13.34 / 12.68	14.21 / 12.92
Mg (Mass/Atom %)	0.48 / 0.25	0.32 / 0.18	0.36 / 0.23	0.30 / 0.18
Al (Mass/Atom %)	0.38 / 0.18	-	0.46 / 0.26	0.13 / 0.07
Si (Mass/Atom %)	0.28 / 0.13	-	-	-
P (Mass/Atom %)	0.35 / 0.14	1.16 / 0.52	1.31 / 0.64	2.48 / 1.16

S (Mass/Atom %)	-	0.30 / 0.13	-	0.29 / 0.13
Cl (Mass/Atom %)	0.39 / 0.14	0.16 / 0.06	0.30 / 0.13	1.08 / 0.44
K (Mass/Atom %)	1.60 / 0.52	7.42 / 2.64	23.07 / 8.97	14.44 / 5.26
Ca (Mass/Atom %)	-	1.13 / 0.39	-	-
Cu (Mass/Atom %)	-	3.44 / 0.75	-	1.60 / 0.37
C/N Ratio (atoms)	-	~183.4	~31.8	~76.1

Based on the data in Table 2, nitrogen is absent in the unmodified AC sample (P1). Elements such as magnesium (Mg), phosphorus (P), silicon (Si), and aluminum (Al) were detected, likely originating from the natural composition of the raw biomass—specifically potato peel residue [21, 22].

For the hydrothermally treated samples (P2, P3, and P4), nitrogen incorporation is evident. Nitrogen levels (by mass) increase to 0.45%, 2.16%, and 0.99%, respectively, as treatment time extends, with corresponding atomic percentages of 0.45%, 2.35%, and 1.03%. Among these, P3 (48-hour treatment) exhibits the highest nitrogen content, which corresponds to the lowest C/N atomic ratio—indicating successful nitrogen doping.

In P4 (72-hour treatment), nitrogen levels decline. This decrease in nitrogen may be attributed to prolonged heating, which could cause nitrogenous compounds such as NH_3 to desorb from internal pores. Alternatively, nitrogen may migrate into the process water during extended hydrothermal exposure.

In terms of atomic percentage, the maximum 2.35% N was in P3. Samples P2-P4 possess very high C/N ratios, ranging from ~31.8 to ~183.4, indicating a carbon-rich but nitrogen-poor structure. Potassium content peaks in P3, potentially due to its adsorption onto the hydrochar surface, resulting in a more thermally stable potassium form under moderate heating conditions. Compared to the okara-derived sample [13, 14], the nitrogen content in the potato-derived sample is much less although of the same treatment time with NH_4OH (48h), which means that nitrogen group may be easier to attach to the structure of AC derived from okara than that of AC derived from potato peel waste.

Chlorine is detected across all samples, including the untreated AC. This likely stems from both residual content in the biomass and the use of HCl during the washing stage of AC sample preparation. The Si and Al (already very low in sample P1) disappeared most probably because low content of Si and Al fell below the detection limit of the analysis equipment (EDX) so not the same at different measurements [23].

The representative EDX spectrum for sample P2 (treated with NH_3 for 48 hours) is shown in Figure 8. This spectrum shows clear evidence of N.

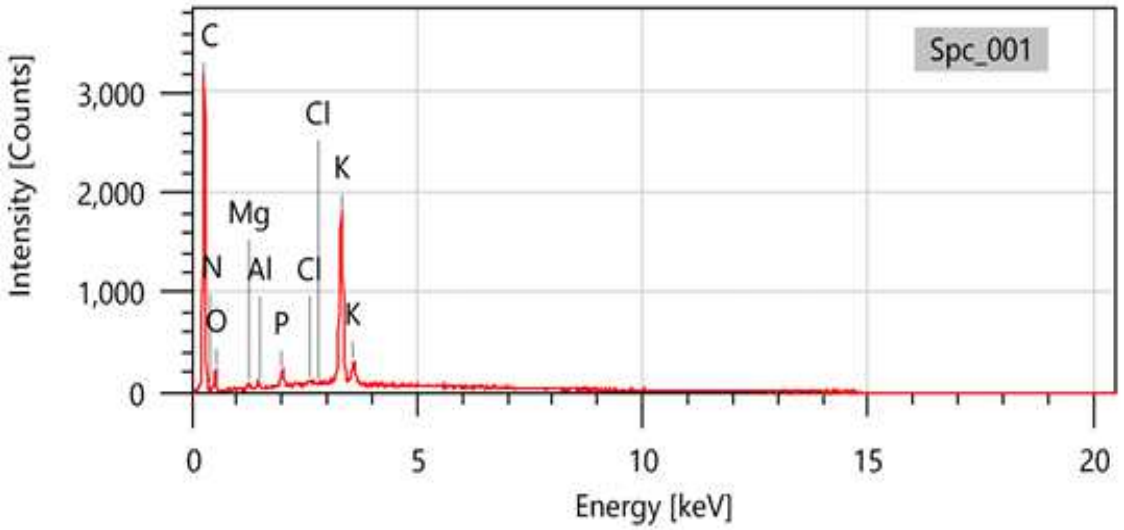

Figure 8. Elemental analysis (EDX) of sample P2 following 48-hour NH_3 treatment

Figure 8 presents the FTIR spectra of the original potato peel-based activated carbon and the sample treated with NH4OH for 48 hours. A broad band near 3457 cm^{-1} in the original AC and 3452 cm^{-1} in the NH_4OH-treated sample corresponds to O-H stretching from hydroxyl groups from absorbed moisture and other functional groups derived from the raw material.

The peak at ~1600 cm^{-1} of the original sample suggests C=C stretching vibrations from aromatic rings, indicating graphitic structures. Peaks around 2361 cm^{-1} for the original AC and 2358 cm^{-1} for the treated AC are linked to O=C=O stretching vibrations. A notable peak at 1618 cm^{-1} in the original AC is attributed to C=C vibrations in aromatic rings of lignin, potentially combined with bending vibrations from adsorbed water.

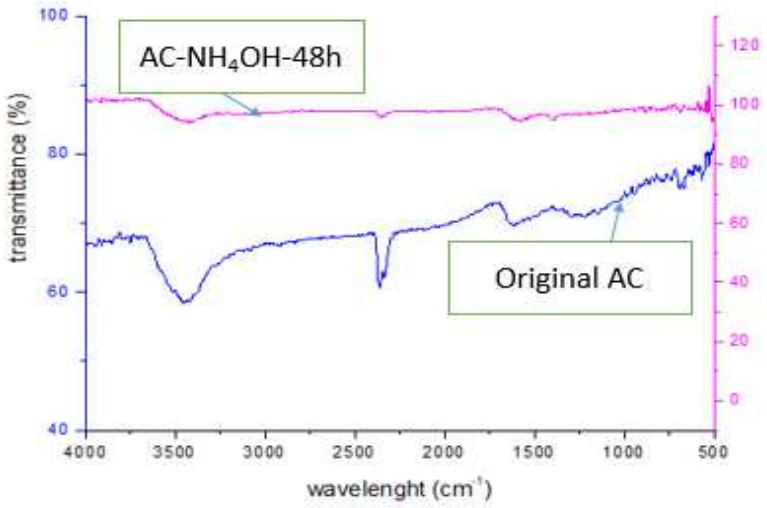

Figure 9. FTIR patterns of the original AC synthesized from potato peels (P1) and AC-NH_4OH-48h

3.3. CO_2 adsorption capacity of the modified potato peel-derived AC

Adsorption performance by TPD CO_2

Figure 10. shows the TPD CO_2 profile of the modified potato peel-derived AC treated with NH_4OH for 48 h (P3). The TPD CO_2 profile of potato peel-derived AC is similar to that of okara-derived AC, showing 2 desorbed peaks at about 100 °C (minor) and 420 °C (major). However, the total CO_2 desorbed is only 1.44 mmol/g, which is even smaller than that of okara-derived AC treated with NH_4OH for half of time (24h).

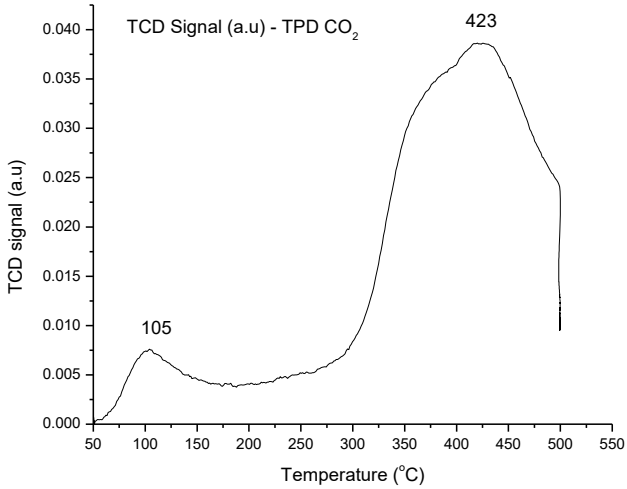

Figure 10. TPD CO_2 profile of the modified potato peel-derived AC.

Adsorption performance by physical adsorption method

CO_2 adsorption results of Modified Potato Peel-derived AC samples were also measured by the physical adsorption method. CO_2 physical adsorption measurement was performed using the Gemini VII 2390 V1.02 device. Firstly, the samples were pre-dried at 105 ºC for 12 hours, then were degassed in a vacuum at 150 ºC for 6 hours to remove all water and surface-adsorbed impurities. The adsorption performance was compared with that of the modified okara-derived AC sample (S3), which was prepared by the same synthesis procedure from the okara-derived AC with 594 m^2/g and possessing a C/N atom ratio of 13.74 [13].

Adsorption performance at room temperature

The CO_2 adsorption process is carried out at room temperature and absolute pressure from 89 - 1000 mmHg, corresponding to a relative pressure range P/P0 from 0.05 to 0.6. The quantity of adsorbed CO_2 was recorded as cm^3/g at standard temperature and pressure. The quantity of adsorbed CO_2 was also calculated to mmol/g by 1 cm^3/g. = 1:22.4141 mol/g = 0.04464 mmol/g (STP condition: 273.15 K. 100kPa). Results of this measurement are provided in Table 3 and Figure 11 below:

Table 3. CO_2 adsorption by physical adsorption measurement method

Absolute pressure (mmHg)	**Potato peel waste 48 h (P3)**		**Okara powder waste 48h (S3)**	
	Quantity Adsorbed (cm^3/g STP)	Quantity Adsorbed (mmol/g)	Quantity Adsorbed (cm^3/g STP)	Quantity Adsorbed (mmol/g)
88.914635	2.26218	0.1010	3.63228	0.1622
177.015610	3.93483	0.1757	5.6164	0.2508
353.459808	5.54226	0.2474	7.69224	0.3433
528.900085	6.56146	0.2927	9.2286	0.4118
704.750610	6.95795	0.3106	9.9744	0.4451
880.207947	7.388752	0.3297	10.712047	0.4786

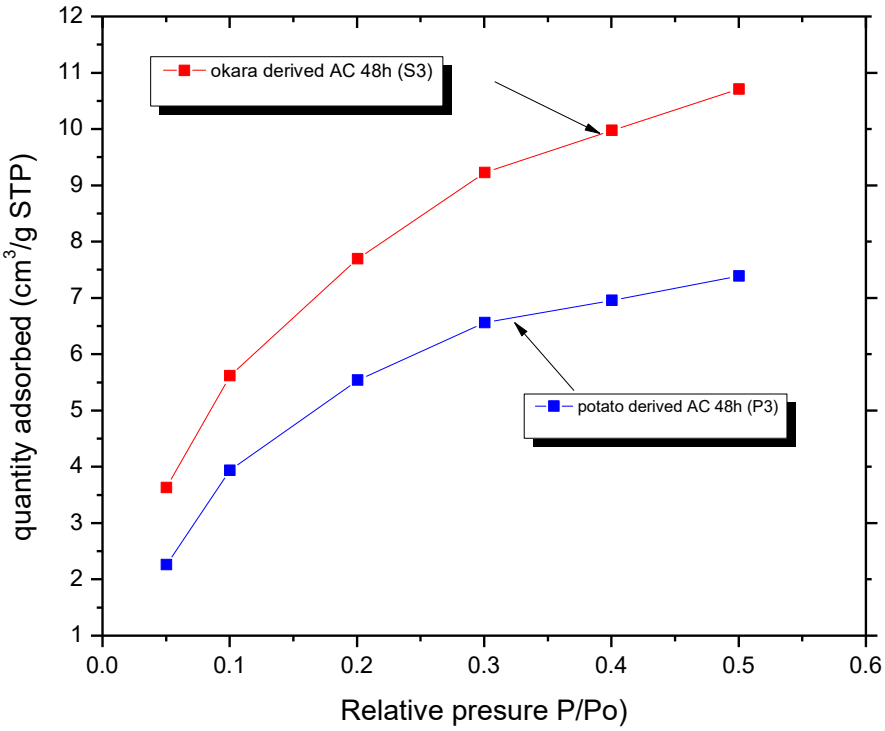

Figure 11. CO_2 adsorption by physical adsorption measurement method at room temperature of potato peel waste 48h (S3) sample and okara powder waste 48h (P3) sample.

The CO_2 adsorption capacities of the samples ranged from 0.101 to 0.478 mmol g^{-1}. The gradual increase in the amount adsorbed with rising pressure indicates a progressive filling of available adsorption sites and micropores. The highest adsorption value of approximately 0.478 mmol g^{-1} for okara sample suggests that the material exhibits modest CO_2 uptake capacity under the tested conditions, which may be attributed to its surface chemistry and pore structure. The CO_2 adsorption isotherm (Figure. 11) shows the relationship between the quantity adsorbed and relative pressure (P/P_0) for two samples: potato peel waste (48h) and okara powder waste (48h). Across the measured pressure range (absolute pressure from 89 - 1000 mmHg), the okara powder waste consistently adsorbs slightly more CO_2 than the potato peel waste. The potato peel waste shows a maximum uptake of approximately 0.329 mmol g^{-1} while the okara sample reaches near 0.4786 mmol g^{-1} These results suggest that despite similar preparation time (48h), the okara-derived adsorbent exhibits enhanced CO_2 affinity, likely due to differences in surface chemistry and porosity resulting from its NH-functional group composition. This result is in a good agreement

with the TPD CO_2 results. However, compared to the chemical CO_2 adsorption capacities of the okara samples, these physical CO_2 adsorption capacities are much smaller. This may prove that the CO_2 adsorption in AC modified with NH- functional groups is mainly chemical adsorption due to the presence of NH- functional groups.

Table 4. Langmuir and Freundlich isotherm parameters for CO_2 adsorption

Sample	Model	Parameters	R2
P3	Langmuir	qmax = 0.434 mmol/g	0.9979
	Freundlich	n = 1.97	0.9610
S3	Langmuir	qmax = 0.613 mmol/g	0.9985
	Freundlich	n = 2.14	0.9851

The equilibrium adsorption data were further analyzed using Langmuir and Freundlich isotherm models as indicated in Table 4. The Langmuir model exhibited higher correlation coefficients for both P3 and S3 samples, suggesting possible monolayer adsorption behavior within the investigated pressure range. In addition, the Freundlich constant n values greater than 1 indicated favorable CO_2 adsorption on the developed biomass-derived ACs.

Adsorption performance measured at 0 °C

CO_2 adsorption measurements were carried out at 0 °C to better evaluate the presence of narrow micropores and ultra-micropores in the prepared ACs. As shown in Figure 12, the amount of CO_2 adsorbed increases steadily with increasing relative pressure (P/P_0) for both samples, the potato peel-derived AC (P3) and okara-derived AC (S3). P3 exhibits a significantly higher adsorption capacity compared with S3 over the entire pressure range investigated. At P/P_0, the entire uptake of P3 reaches approximately 40 cm^3/g STP**,** while that of S3 is about 20 cm^3/g STP**.**

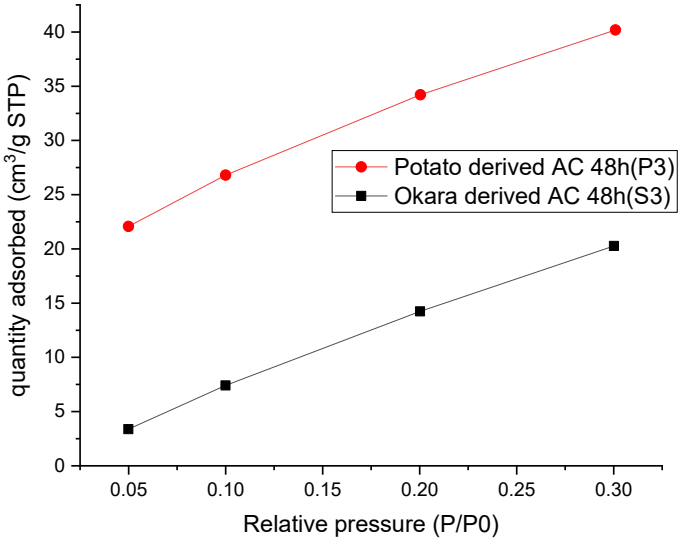

Figure 12. Adsorption measured at 0 °C

The adsorption behavior observed at 0 °C is mainly associated with the presence of narrow micropores and ultra-micropores (<1 nm) in the carbon structure, which provide strong confinement effects for CO_2 molecules with a kinetic diameter of about 0.33 nm**.** These results suggest that the pore structure developed in the potato-peel-derived activated carbon is more favorable for CO_2 adsorption compared with that of the okara-derived material.

Table 5. CO_2 adsorption by physical adsorption measured at 0 °C

Potato peel waste 48 h (P3)			**Okara powder waste 48h (S3)**		
Relative Pressure (P/Po)	Quantity Adsorbed (cm^3/g STP)	Quantity Adsorbed (mmol/g)	Relative Pressure (P/Po)	Quantity Adsorbed (cm^3/g STP)	Quantity Adsorbed (mmol/g)
0.04996	5.817978	0.260	0.049926	3.376613	0.151
0.100032	10.53945	0.470	0.099977	7.411158	0.331
0.20043	17.95287	0.801	0.200256	14.23906	0.635
0.300941	23.93351	1.068	0.30016	20.26703	0.904

The CO_2 adsorption isotherms measured at 0 °C show that the amount of adsorbed CO_2 increases steadily with increasing relative pressure (P/P_0) for both samples. As shown in Table 5, for S3, the adsorption capacity increases from approximately 0.15 mmol g^{-1} at P/P_0 at P/ to about 0.90 mmol g^{-1} at P/P_0 at P/P. In contrast, the P3 exhibits higher adsorption capacities over the entire pressure range, increasing from 0.26 mmol g^{-1} to approximately 1.07 mmol g^{-1} at P/P_0 at P/Po

The higher CO_2 uptake at 0 °C observed for the potato-peel-derived activated carbon may be attributed to its more developed porous structure and larger specific surface area, which provide more adsorption sites for CO_2 molecules. In addition, the narrow micropores present in the carbon framework can enhance the interaction between CO_2 molecules and the adsorbent surface through confinement effects, which is particularly important for CO_2 molecules with a kinetic diameter of about 0.33 nm. However, the opposite observation was seen for the adsorption at room temperature. This suggests that at higher temperatures (room temperature) the chemical adsorption may predominate, as the okara sample contains more nitrogen groups than the potato peel sample, as seen from EDX results.

To determine the adsorption selectivity of CO_2 compared to the other gases, the adsorption performance of N_2 of the okara sample (S3) was also measured at 0 °C as shown in Figure 13.

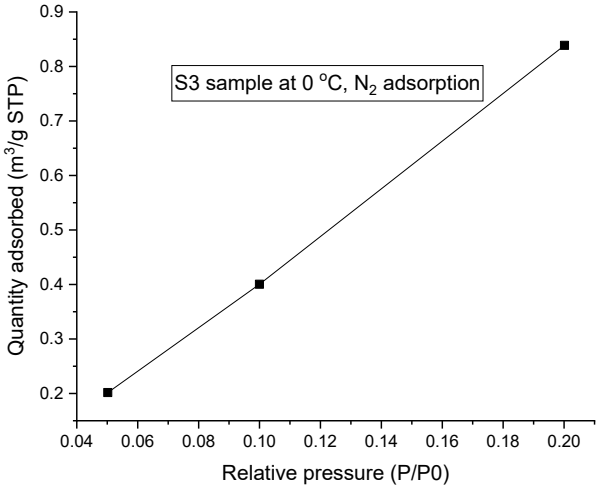

Figure 13. N_2 adsorption capacity of the S3 sample measured at 0 °C

The N_2 adsorption capacity is significantly lower than that of CO_2 over the measured pressure range (adsorption quantity at P/P_0 for the N_2 and CO_2 adsorption are 0.0374 and 0.635

mmol/g, respectively). This can be attributed to the smaller kinetic diameter and higher affinity of CO_2 molecules, which allow more effective diffusion and adsorption within narrow micropores compared to N_2.

3.4.Indication of adsorption and desorption through the production of Na_2CO_3

To prove the adsorption and desorption of CO_2 in the AC sample, firstly, CO_2 was adsorbed on the modified potato peel-derived AC sample, followed by the desorption step occurring in the presence of NaOH solution.

In aqueous alkaline media, absorbed CO_2 can react with NaOH to form carbonate and, depending on the reaction conditions and CO_2 availability, bicarbonate species. The overall conversion can be represented by the following reactions:

$$2NaOH+CO_2 \rightarrow Na_2CO_3 + H_2O$$

In the presence of excess CO_2 or under cooler conditions. The reaction is:

$$NaOH+CO_2 \rightarrow NaHCO_3$$

Therefore, if CO_2 was adsorbed and then desorbed, the desorbed CO_2 will immediately react with NaOH solution to form Na_2CO_3; i.e the formation of Na_2CO_3 proves the presence of adsorbed CO_2 in the sample.

Moreover, sodium carbonate (Na_2CO_3), also known as soda ash or washing soda, is widely used in various industries. In glass manufacturing, about 50%–60% of industrial sodium carbonate is used in making glass. It reduces the melting point of silica (SiO_2), which makes the glass production process more energy-efficient. Na_2CO_3 is used in soda-lime glass, the most common type (e.g., bottles, windows). In construction, Na_2CO_3 is used as an additive to enhance the mechanical strength of PVA/CMC films [24]. Na_2CO_3 is used as a detergent and cleaning agent. In food industry, food-grade Na_2CO_3 is used as a food additive. It functions as a raising agent, acidity regulator, or anti-caking agent. For instance, the addition of 0.20% and 0.25% Na_2CO_3 resulted in a finer and smoother dough texture [25]. Therefore, the CO_2 adsorption and desorption on modified AC to form Na_2CO_3 may also be an application for the utilisation of CO_2.

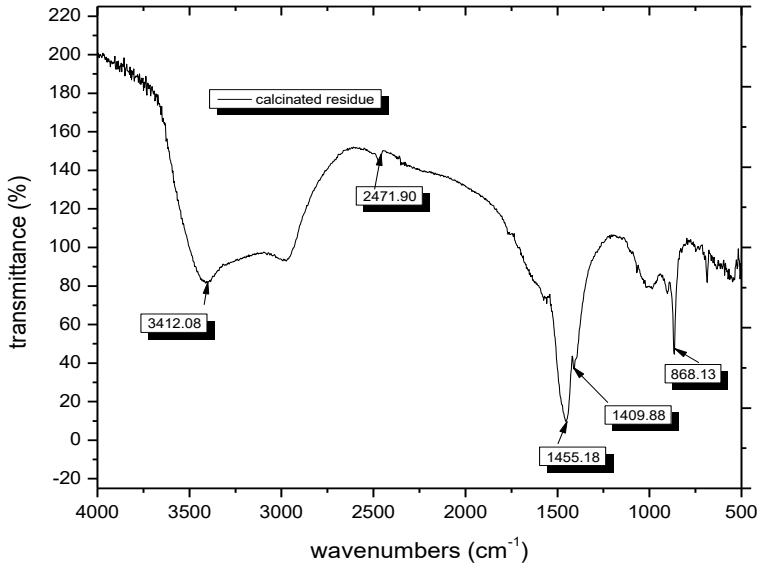

Figure 14. FTIR of R1 residue

FTIR analysis of the residues R1 is shown in Figure 14. The evaporated residue R1 is in a white, hygroscopic solid. The FTIR spectrum in Figure 14 above does show the presence of the carbonate ion (CO_3^{2-}) through the bands at 1455.18 & 1409.88 (presented the Asymmetric stretching ν_3), 868.13 (presented the Out-of-plane bending ν_2), 985.23 and 902.91 (presented possibly in-plane bending ν_4 or combination bands). The FTIR of evaporated residue also shows that a peak at 3412.08 cm^{-1} attributes to broad O–H stretching, likely from adsorbed water. At 2471.90 cm^{-1} wavenumber, this is possibly CO_2 or bicarbonate contamination. At fingerprint region (~500–400 cm^{-1}), complex bending modes, present in metal carbonates. The result confirms CO_2 capture by AC has been reacted with NaOH solution to form Na_2CO_3.

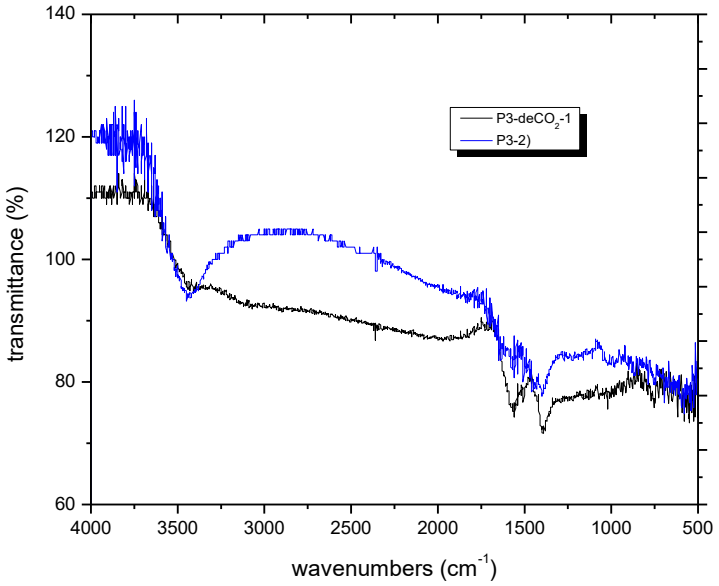

Figure 15. FTIR of P3-deCO₂-1 sample (after CO₂ adsorption) and P3-2 sample (after reaction with NaOH solution.

FTIR of AC samples (P3) derived from potato peel waste after CO_2 adsorption (noted as P3-deCO₂-1) and after reaction with NaOH solution (noted as P3-2) are presented in Figure 15. In these samples, the bands belonging to CO_3^{2-} are clearly seen in the region 1410–1470 cm^{-1}, confirming that CO_2 is present in these samples. However, the intensity of these bands in the sample after reaction with NaOH solution (P3-2) is smaller than that in the sample before the reaction with NaOH solution (P3-deCO₂-1), proving that CO_2 has been desorbed partly and reacted with NaOH solution to form Na_2CO_3.

The residue sample R1 above is also analyzed by XRD techniques to identify Na_2CO_3. The result of the XRD analysis of this sample is shown in Figure 16 below (red spectrum). Alternatively, to confirm whether the conversion by NaOH solution took place in this experiment, a blank sample in which only 0.64 g NaOH powder (no AC) is diluted with 20 mL H_2O was prepared. The solution is then heated and evaporated at 140 ^oC. Then the residue is kept in an oven of 110-120 ^oC overnight. XRD of this sample is also shown in Figure 16 (black spectrum). In this red spectrum, there are visible peaks around: ~20.9°, ~29.4°, ~31.7°, ~35.8°, ~39.4°, ~43.0°, ~47.4°. These closely match the standard Na_2CO_3 peaks, strongly suggesting that Na_2CO_3 is present in the sample [26, 27].

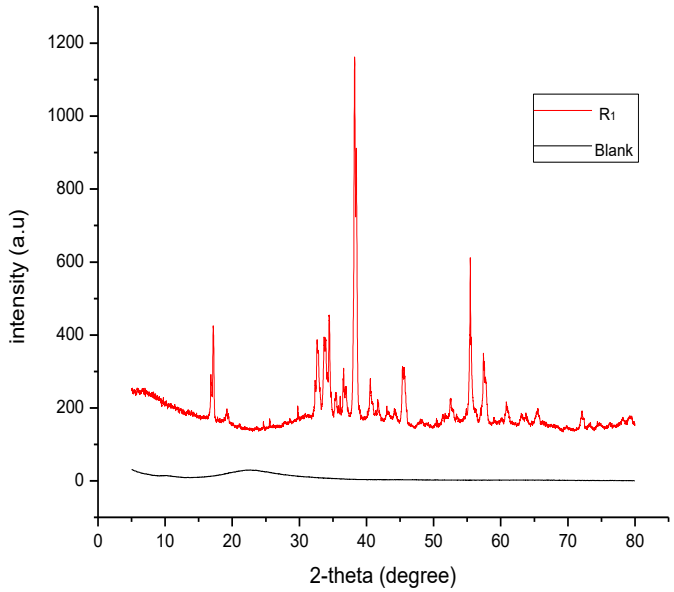

Figure 16. XRD spectra of two samples plotted in one figure

The XRD pattern of the blank sample (black curve) shows a broad, weak hump centered around 20–30° 2θ, with no sharp crystalline peaks. This is a typical XRD signature of an amorphous or poorly crystalline material**.** There are no distinct diffraction peaks corresponding to Na_2CO_3 or any other crystalline phase. Therefore, no evidence of Na_2CO_3 can be identified from this XRD pattern.

4. Conclusions

This study focused on potato peel waste, in comparison with okara potato waste, abundant in Asia and inexpensive to collect, as a feedstock for porous carbon synthesis. Using slow pyrolysis, porous activated carbon was successfully produced and used to adsorb CO_2 after modification with ammonia. After KOH activation, the potato-peel-derived activated carbon exhibited a higher surface area, reaching up to 969 m^2/g. However, despite the larger surface area, ammonia modification resulted in relatively low nitrogen incorporation compared to the okara-derived materials. EDX analysis of potato-peel-derived activated carbon impregnated with NH_4OH for 48 h confirmed the highest nitrogen content of approximately 2.16 wt%. Nevertheless,

due to the lower nitrogen functionalization compared with the okara-derived materials, the CO_2 adsorption capacity remained lower, reaching approximately 1.44 mmol/g for the 48 h ammonia-impregnated sample.

In addition to adsorption studies, CO_2 conversion using NaOH solution was successfully demonstrated. FTIR and XRD analyses confirmed the formation of Na_2CO_3, indicating the potential for integrating CO_2 capture and conversion within a single system. Although research on CO_2 conversion to Na_2CO_3 is still at an early stage, it confirms the potential for industrial applications.

In conclusion, agricultural residues such as okara and potato peels can be transformed into functional porous ACs for CO_2 capture. While their adsorption capacities are moderate, continued refinement of synthesis methods and functionalization methods may yield scalable, sustainable solutions to support climate mitigation, circular economy goals, and Net Zero commitments.

Supplementary Information

Supplementary material is available upon request.

Author Contributions

Tuan-Dung Hoang contributed to methodology, conceptualization, data curation, resources, investigation, visualization, formal analysis, and writing the original draft. Minh Thang Le was involved in supervision, review, and editing. All authors have read and approved the final manuscript.

Data availability

The authors confirm that the data supporting the findings of this study are available in the paper. Raw data supporting the findings of this study are available from the corresponding author upon request.

Funding Declaration

Not applicable

Acknowledgment

Not applicable

Ethics, Consent to Participate, and Consent to Publish Declarations

Ethics, Consent to Participate, and Consent to Publish declarations: Not applicable.

Clinical Trial Registration

Not applicable. This study did not involve a clinical trial.

Declarations Competing interests

The authors declare no competing interests.

References

1. Khedulkar, A.P., et al., *Bio-based nanomaterials as effective, friendly solutions and their applications for protecting water, soil, and air.* 2025. **46**: p. 102688.
2. Abi Bianasari, A., et al., *Influence of combined catalysts on the catalytic pyrolysis process of biomass: A systematic literature review.* 2024. **309**: p. 118437.
3. Sepelev, I. and R. Galoburda, *Industrial potato peel waste application in food production: a review.* Food science, 2015.
4. Wu, D.J.P.E.S., *Recycle technology for potato peel waste processing: A review.* 2016. **31**: p. 103-107.
5. Calıskan, M.E., A. Bakhsh, and K. Jabran, *Potato production worldwide*. 2022: Academic Press.
6. Zhang, Z., et al., *Enhancement of CO2 adsorption on high surface area activated carbon modified by N2, H2 and ammonia.* Chemical Engineering Journal, 2010. **160**(2): p. 571-577.
7. Pevida, C., et al., *Surface modification of activated carbons for CO2 capture.* Applied Surface Science, 2008. **254**(22): p. 7165-7172.
8. Heidari, A., et al., *Evaluation of CO2 adsorption with eucalyptus wood based activated carbon modified by ammonia solution through heat treatment.* Chemical Engineering Journal,, 2014. **254**: p. 503-513.
9. Pevida, C., et al., *Surface modification of activated carbons for CO2 capture.* 2008. **254**(22): p. 7165-7172.
10. Abd, A.A., et al., *A review on application of activated carbons for carbon dioxide capture: present performance, preparation, and surface modification for further improvement.* Environmental Science and Pollution Research, 2021. **28**(32): p. 43329-43364.
11. Yin, Q., M. Liu, and H.J.B. Ren, *Removal of ammonium and phosphate from water by Mg-modified biochar: Influence of Mg pretreatment and pyrolysis temperature.* BioResources, 2019. **14**(3): p. 6203-6218.
12. Xiong, Z., A.K. Sarmah, and L.P.J.S.o.T.T.E. Padhye, *Acidic surface functional groups control chemisorption of ammonium onto carbon materials in aqueous media.* Science of The Total Environment, 2020. **698**: p. 134193.

13. Hoang, T.-D., Y. Liu, and M.T.J.P. Le, *Performance of CO2 adsorption on modified activated carbons derived from Okara powder waste: impacts of Ammonia impregnation.* 2024. **12**(9): p. 2024.
14. Hoang, T.-D., Y. Liu, and M.T.J.S. Le, *Synthesis and characterization of biochars and activated carbons derived from various biomasses.* 2024. **16**(13): p. 5495.
15. Nguyen, H.N., et al., *Experimental investigation of CO2 adsorption using adsorbents derived from residual char of agricultural waste gasification.* Thermal Science and Engineering, 2024. **49**: p. 102446.
16. Vu, N.L., et al., *Exploring adsorbent potential: Investigating the characteristics of macadamia husk char from pilot-scale gasification.* Vietnam Journal of Catalysis and Adsorption, 2024. **13**(4): p. 20-25.
17. Thuy, L.T.T.J.J.o.S.N.S., *STUDY ON THE CO\(_2\) ADSORPTION PROPERTIES OF ACTIVATED CARBON PRODUCED FROM CORN COB.* 2024: p. 78-89.
18. Coromina, H.M., D.A. Walsh, and R.J.J.o.M.C.A. Mokaya, *Biomass-derived activated carbon with simultaneously enhanced CO 2 uptake for both pre and post combustion capture applications.* Journal of Materials Chemistry, 2016. **4**(1): p. 280-289.
19. Vali, I.P., et al., *Bamboo and coconut shell based activated carbon: a Raman spectroscopic study.* Materials Chemistry and Physics,, 2024. **318**: p. 129240.
20. Patil, P., et al., *Enhanced adsorption of phenolic compounds using biomass-derived high surface area activated carbon: Isotherms, kinetics and thermodynamics.* Environmental Science and Pollution Research, 2024. **31**(60): p. 67442-67460.
21. Wang, T., et al., *What is the influence of the nitrogen-containing composition during hydrothermal carbonization of biomass? A new perspective from mimic feedstock.* Bioresource Technology 2019. **5**: p. 343-350.
22. Leng, L., et al., *A review on nitrogen transformation in hydrochar during hydrothermal carbonization of biomass containing nitrogen.* Science of the Total Environment, 2021. **756**: p. 143679.
23. Ghani, U., et al., *Hydrothermal extraction of amorphous silica from locally available slate.* ACS omega, 2022. **7**(7): p. 6113-6120.
24. Zhu, J., et al., *Effect of Na2CO3 on the microstructure and macroscopic properties and mechanism analysis of PVA/CMC composite film.* Polymers, 2020. **12**(2): p. 453.
25. Sun, X., et al., *Influence of Na2CO3 on the quality of dough with rice wine sourdough and steamed bread.* International Journal of Food Science and Technology, 2020. **55**(5): p. 2261-2270.
26. Oh, S.Y., et al., *Crystalline structure analysis of cellulose treated with sodium hydroxide and carbon dioxide by means of X-ray diffraction and FTIR spectroscopy.* Carbohydrate research,, 2005. **340**(15): p. 2376-2391.
27. Simanjuntak, W., et al., *The use of carbon dioxide released from coconut shell combustion to produce Na2CO3.* Makara J. Sci 2014. **18**(3): p. 1.